Partial Grid Forming Concept for 100% Inverter-Based Transmission Systems

Uros Markovic*, Ognjen Stanojev*, Petros Aristidou§, Gabriela Hug*

* EEH - Power Systems Laboratory, ETH Zurich, Physikstrasse 3, 8092 Zurich, Switzerland
§ School of Electronic and Electrical Engineering, University of Leeds, Leeds LS2 9JT, UK
Emails: {markovic, hug}@eeh.ee.ethz.ch, ognjens@student.ethz.ch, p.aristidou@leeds.ac.uk

Abstract—With the current trends in renewable energy integration, the concept of a 100% inverter-based power system is becoming more of a reality. However, the existing Voltage Source Converter (VSC) control schemes for such systems focus mostly on the operation of low-voltage microgrids, which have different requirements from the transmission system perspective. This paper proposes a new classification of VSC control strategies depending on their mode of operation. Then, the concept of partial grid forming VSC is introduced and it is shown that a system with zero rotational inertia can operate without a dedicated grid-forming VSC unit, but rather with partial forming of key system characteristics distributed across different VSC units. The performance of this approach is tested on detailed VSC models developed in both MATLAB Simulink and virtual Hardware-In-the-Loop (vHIL) platforms. Furthermore, an investigation towards necessary converter and network criteria for providing a stable system under the proposed control concepts is presented.

Index Terms—voltage source converter (VSC), grid-forming, grid-following, grid-supporting, partial system forming

I. INTRODUCTION

Power systems are currently facing a major transition from large Synchronous Machines (SMs) to smaller generation units, interfaced via Voltage Source Converters (VSCs). The presence of existing SMs still allows for the majority of inverter-based generation to be controlled as *grid-following* (also termed *grid-feeding*) units [1]–[3]. Nevertheless, this mode of operation relies heavily on the assumption of a stiff AC grid and accurate tracking of the already formed frequency and voltage; this assumption collapses in the case of systems with 100% Power Electronics (PE) penetration. Hence, several *grid-forming* control strategies have been proposed that provide certain SM-like properties to the VSCs, such as standalone and black-start mode of operation, frequency and voltage support, and synchronization capabilities [4], [5]. The forming aspect of VSC control has been mostly addressed in the context of microgrids, where frequent configuration changes can result in switching between the grid-connected and islanded mode of operation [6]–[8].

Due to the nature of the problem, all of the proposed approaches distinguish between a forming and a following mode of the VSC control; with the first one solely establishing the voltage magnitude and frequency in the system, and the latter providing predefined power to the energized grid. An extension to this categorization was presented in [9], where a new class of VSC control mode was defined and named *grid-supporting*. Essentially, it is a modification of the first two modes, with incorporation of additional high-level control loops that enable regulation of an AC voltage vector via power output. Since a grid-supporting VSC can be represented either as a voltage or a current source, it possesses standalone capabilities only under certain control configurations.

However, this somewhat general classification is quite restrictive for the multifaceted nature of the problem, and occasionally unclear, as similar terms are used across the literature for different VSC concepts, as in case of a grid-supporting model presented in [10]. Furthermore, all of the proposed configurations assume that a converter is either forming both the voltage and frequency in the system, or measuring them via a Phase-Locked Loop (PLL) unit. While this might prove sufficient for low-voltage microgrids, it is not necessarily optimal for VSC control on a transmission system level, as shown in [11].

The concept of a large-scale power system with high PE penetration is now becoming a reality [12], which makes the inadequacy of current VSC mode classification even a greater problem. Several studies have addressed the requirements for 100% inverter-based power systems, with a focus mostly on new control architecture and ancillary services [13], [14], as well as the feasibility criteria under various operational scenarios [15]. However, all of the conclusions have been drawn under the premise of a converter operating either as a grid-forming or grid-following unit. While a need for a more versatile control categorization has been indicated in [14], no solution has been suggested thus far.

The contribution of this work is three-fold. First, we propose a new, more comprehensive, classification for control strategies of VSCs. The concept of *partial* grid-forming control strategy is introduced and it is shown that a 100% PE-interfaced system can operate without a dedicated grid-forming unit, but rather with partial forming of individual system parameters distributed across different converter units. Second, we test the performance of this approach using a detailed VSC model with a state-of-the-art control structure, developed in both MATLAB Simulink and virtual Hardware-In-the-Loop (vHIL) platforms. Finally, we investigate the necessary conditions and grid configuration criteria for providing a stable system under

the proposed approach.

The remainder of the paper is structured as follows. In Section II, the concept of partial grid forming is introduced, together with the new converter mode classification. Section III describes the VSC model used in this paper. Section IV compares the transient response of different partial forming configurations and investigates the necessary stability requirements, whereas Section V discusses the outlook of the study and concludes the paper.

II. PARTIAL GRID FORMING

The proposed classification in [9] distinguishes between VSCs controlled as a voltage or a current source, with grid-forming being the first and grid-following the latter type. The grid-supporting mode can fall into both categories, as it is conceptually based on the previous two schemes with incorporation of the droop control. According to the capability of individually establishing the voltage vector, all three proposed control modes may either use both the voltage magnitude and frequency setpoints, or none. However, from the perspective of the power system operation, these two characteristics are controlled independently. Furthermore, in order to obtain a system-level categorization of the VSC operation modes, it is important to make them independent of the particular device-level implementation.

One way to classify the system-level specifications is by differentiating between which of the two voltage vector variables (magnitude v and frequency ω) are regulated to constant values and which ones vary according to locally measured signals. In other words, the voltage reference signals can be defined either as constant setpoints (v_0, ω_0) or as measurements inputs ($\tilde{v}$, $\tilde{\omega}$), which yields four possible converter operation modes:

1) Grid-forming (g-form): Establishes a complete voltage vector, similarly to the grid-forming model in [9]: $[v^*, \omega^*]$.

2) Frequency-forming (f-form): Independently forms the frequency, while the voltage magnitude follows the measured reference: $[\tilde{v}, \omega^*]$.

3) Voltage-forming (v-form): Forms the magnitude of the voltage at the Point of Common Coupling (PCC), and synchronizes it accordingly via a PLL unit: $[v^*, \tilde{\omega}]$.

4) Grid-feeding (g-feed): Voltage vector is completely dependent on the local measurements: $[\tilde{v}, \tilde{\omega}]$.

In order to make the categorization completely independent of the local control, we consider a unified VSC configuration for all proposed unit types, with active and reactive power being regulated through means of droop control. This is also another distinction from [9], where a grid-forming unit is not controlling the power output.

This classification allows to describe the situation where partial forming VSCs are used to operate the system, with voltage magnitude and frequency being independently formed at different locations in the grid. Such approach indicates that a 100% inverter-based network can operate without a dedicated grid-forming unit, which has not been considered feasible thus far.
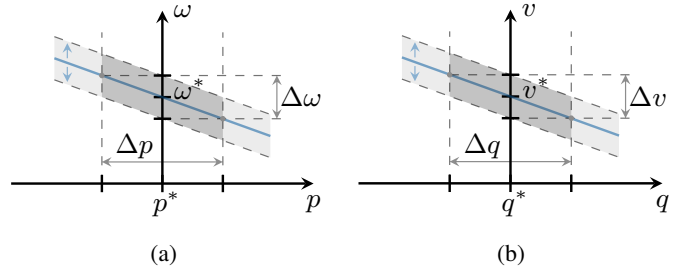

Fig. 1: Impact of a time-varying reference on droop characteristics: (a) active power droop; (b) reactive power droop.

III. VSC CONTROL SCHEME

An overview of the VSC model used in this work is shown in Fig. 2, consisting of an ideal DC voltage source, interfaced through a DC/AC converter and an RLC filter to the grid. The control scheme contains an outer loop which uses the voltage and current measurements to compute the desired voltage magnitude and frequency by means of active and reactive power controllers. These signals are then passed through the inner control loop consisting of cascaded voltage and current controllers. The model also includes a grid synchronization unit that provides the frequency reference for the outer control.

A. Power Controllers

Having in mind that an inverter-based transmission system is under investigation, it is justified to assume a full decoupling of active power and frequency from the reactive power and voltage terms. Hence, we can employ a standard droop characteristic for regulating the active and reactive power output of the converter in the form of

$$\omega = \omega^* + D_p(p^* - \lambda(s)p) \tag{1}$$
$$v = v^* + D_q(q^* - \lambda(s)q) \tag{2}$$

where p and q denote the active and reactive power measurement, while ω and v refer to the frequency and voltage output of the active and reactive power controller, respectively; superscript $*$ indicates a respective reference value. The droop slopes D_p and D_q are imposed on the mismatch between a predefined reference and an actual power measurement, passed through a first-order Low-Pass Filter (LPF)

$$\lambda(s) = \frac{\omega_c}{\omega_c + s} \tag{3}$$

with ω_c being the cutoff frequency. In the case of measurements being used as reference inputs, the droop curve might oscillate as the respective variable varies, providing an operating range depicted as shaded region in Fig. 1. Based on the computed frequency ω, a corresponding phase angle θ needed for the (dq)-transformation is determined.

B. Synchronization Unit

The synchronization unit provides an adequate frequency reference to the outer control loop. In case of a g-form and f-form VSC this is just a constant setpoint ω_0, whereas a PLL measurement ω_{pll} is used otherwise. For this purpose,
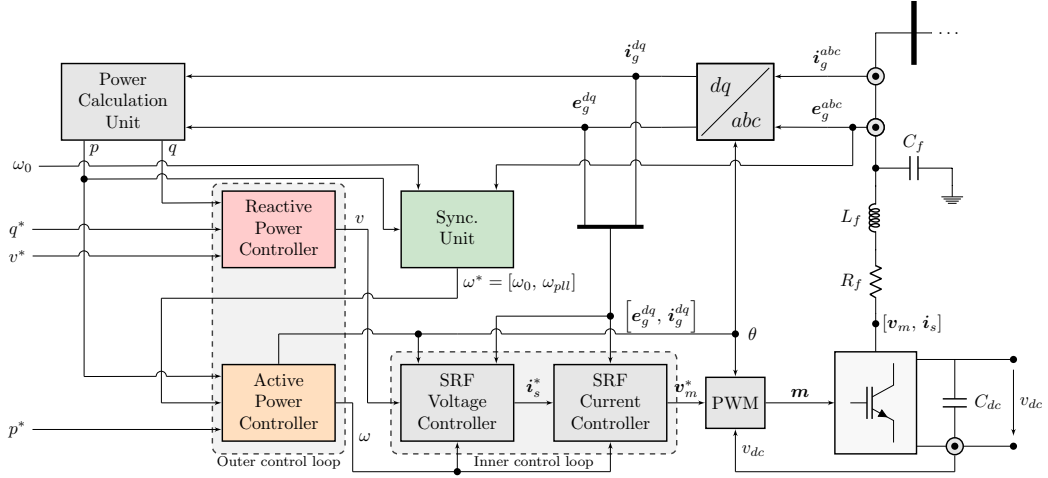
Fig. 2: General configuration of the proposed VSC control structure.

a Type-2 PLL operating in a Synchronous Reference Frame (SRF) has been implemented [16], which is based on the (dq)-transformation of a balanced three-phase voltage signal e_g^{abc} with a magnitude $\hat{e}_g$ and a frequency $\hat{\omega}$:

$$e_g^{dq} = \boldsymbol{T}_p \boldsymbol{T}_c e_g^{abc} = \hat{e}_g \begin{bmatrix} \cos\left(\hat{\theta} - \theta_{pll}\right) \\ \sin\left(\hat{\theta} - \theta_{pll}\right) \end{bmatrix} \quad (4)$$

with $\hat{\theta} = \int \hat{\omega} dt$ and $\theta_{pll} = \int \omega_{pll} dt$, as well as $\boldsymbol{T}_c$ and $\boldsymbol{T}_p$ denoting the Clarke and Park transformation matrices. The synchronization is achieved by initially aligning the d-axis of SRF with the voltage vector, hence diminishing the q-component. Reasonably assuming $\hat{e}_g \approx 1$, this would equate to $\sin\left(\hat{\theta} - \theta_{pll}\right) \approx 0$, i.e. $\hat{\theta} \approx \theta_{pll}$. The PLL is implemented as a PI controller of the phase angle difference, treating it as an error signal and driving it to zero:

$$\omega_{pll} = \omega_0 + \left(K_p^{pll} + \frac{K_i^{pll}}{s}\right) e_g^q \quad (5)$$

C. Inner Control Loop and Modulation

The structure of the inner loop controllers follows the same principles as in [9], [11], and can be described through a cascade computation of the (dq) reference vectors for the switching current $\boldsymbol{i}_s^*$ and modulation voltage $\boldsymbol{v}_m^*$ as:

$$\boldsymbol{i}_s^* = K_f^i e_g + (\boldsymbol{v} - e_g)\left(K_p^v + \frac{K_i^v}{s}\right) + \omega C_f \hat{e}_g \quad (6)$$

$$\boldsymbol{v}_m^* = K_f^v e_g + (\boldsymbol{i}_s^* - \boldsymbol{i}_g)\left(K_p^i + \frac{K_i^i}{s}\right) + \omega L_f \hat{\boldsymbol{i}}_g \quad (7)$$

where $\hat{\boldsymbol{i}}_g = \left[-i_g^q, i_g^d\right]^T$ and $\hat{\boldsymbol{e}}_g = \left[-e_g^q, e_g^d\right]^T$, while K_p, K_i and K_f are the proportional, integral and feed-forward gains, respectively; superscripts v and i denote the voltage and current SRF controllers. The generated voltage reference is combined with the DC-side voltage in order to determine the final (abc) vector of the modulation signal $\boldsymbol{m}^{abc}$ as follows:

$$\boldsymbol{m}^{abc} = (\boldsymbol{T}_p \boldsymbol{T}_c)^{-1} \boldsymbol{m}^{dq} = (\boldsymbol{T}_p \boldsymbol{T}_c)^{-1} \frac{\boldsymbol{v}_m^*}{v_{dc}} \quad (8)$$

IV. RESULTS

In this section, feasibility of the proposed VSC operation modes is investigated through transient responses. Additionally, different system conditions and network parameters are considered in order to reflect important properties of the proposed configurations. For this purpose, a converter model was implemented in two different platforms: (i) an averaged VSC model in MATLAB Simulink with the use of the Sim-PowerSystems toolbox; and (ii) a detailed three-phase inverter with full switching in vHIL platform from Typhoon HIL [17]. The latter one is a software toolbox within a HIL toolchain that enables HIL models to run on a local computer instead of a HIL device. It is not a simulator, but rather a true HIL emulator that runs the same code of the HIL processor and communicates with the same HIL toolchain. Therefore, it provides us with a higher degree of accuracy regarding the performance of the developed control strategies.

The nominal parameters of the VSCs are as follows: AC voltage $V_n = 320\,\text{kV}$; DC voltage $V_{dc} = 640\,\text{kV}$; active power $P_n = 1\,\text{GW}$; and frequency $f_n = 50\,\text{Hz}$.

A. VSC Interactions

In this section, we investigate the 2-bus system depicted in Fig. 3, under all possible configuration scenarios listed in Table I; the green and red fields indicate if a scenario is stable or not. Each converter is connected through a transformer (R_{tr}, L_{tr}), with a transmission line in between the two nodes (R_t, L_t, C_t), and a resistive load (R_l) supplied at the first bus.

As expected, it is confirmed that only scenarios involving the forming of both voltage magnitude and frequency are stable. Furthermore, the simulations also show that the partial forming of individual network parameters (scenarios S_{23} and
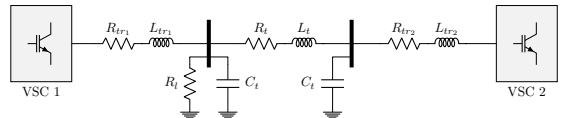

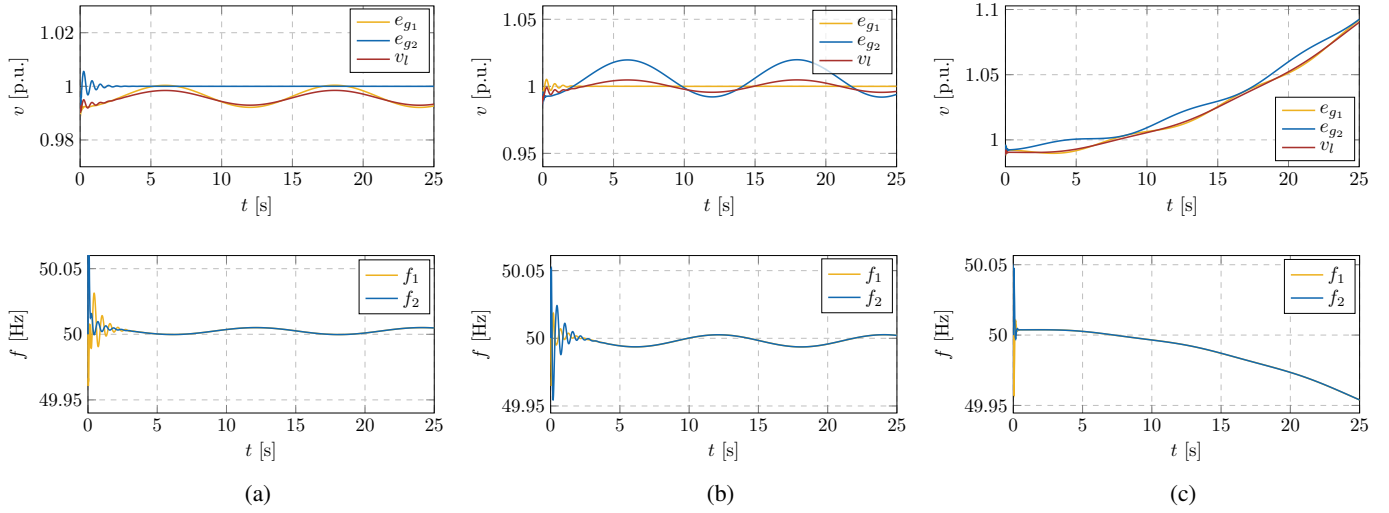Fig. 3: Configuration of the investigated 2-bus system.

Fig. 4: Interactions between VSCs under different configuration scenarios: (a) S_{23}; (b) S_{32}; (c) collapse in S_{22} and S_{33}.

S_{32}) results in a sustainable system, as presented through system dynamics in Fig. 4a and Fig. 4b. For simplicity and clarity of the results, only MATLAB responses are considered.

In both cases, the converter aligns the non-formed variable according to the output provided by the other unit; f_2 follows f_1, while e_{g_1} follows e_{g_2} in scenario S_{23}, and vice versa in scenario S_{32}. Since frequency is a global variable, the synchronization of VSCs is achieved with an adequate accuracy. However, the voltage mismatch is more drastic, as it incorporates a voltage drop between the bus with a fixed voltage reference, and the one where it is being measured. The oscillatory nature of the response is a consequence of the droop characteristic elaborated in Section III.

System dynamics in scenarios S_{22} and S_{33} also indicate that the non-formed variables tend to align with the measurement, as shown in Fig. 4c for the voltage magnitude in S_{22} and frequency in S_{33}, respectively. However, in the absence of a fixed setpoint, none of these quantities converge to a steady state. The system instability under high load demand conditions also prevails in certain scenarios, denoted with light green color in Table I, as will be further elaborated.

B. Provision of Power Reserves

In order for the system to be stable, the load demand must be met at all times. However, depending on the VSC mode, some units might not be responsive to sudden load changes, but rather follow the predefined power setpoints. Essentially, a converter reacts to a change in active power demand only if it *forms* the frequency, i.e. falls under g-form or f-form category. Similarly, a reactive power regulation is only provided by g-form and v-form units. On that note, if the cumulative available

TABLE I: Scenario Stability Results

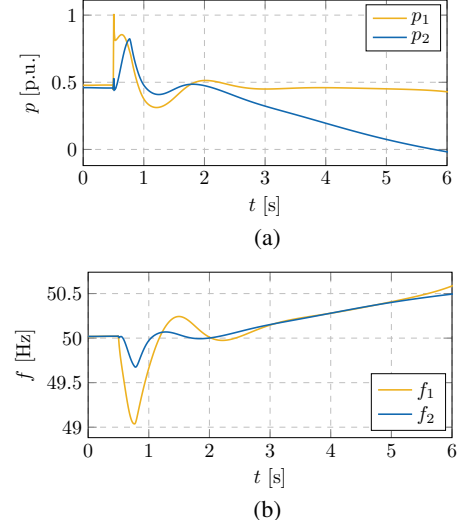| VSC 1 \ VSC 2	g-form	f-form	v-form	g-feed
g-form	S_{11}	S_{12}	S_{13}	S_{14}
f-form	S_{21}	S_{22}	S_{23}	S_{24}
v-form	S_{31}	S_{32}	S_{33}	S_{34}
g-feed	S_{41}	S_{42}	S_{43}	S_{44}

Fig. 5: System collapse in case of insufficient active power reserves from an f-form VSC: (a) active power; (b) frequency.

power reserves of all g-form and f-form VSCs in the system do not meet the active load requirements, the system will collapse. An example of such incident for scenario S_{32} is shown in Fig. 5, where an f-form unit tries to meet the increase in demand, but fails due to insufficient capacity; v-form VSC is unresponsive.

C. Sensitivity Analysis

As previously suggested, the length of a transmission line has a direct impact on the voltage drop, and hence the respective oscillations. For that reason, we have conducted a sensitivity analysis for scenarios S_{23} and S_{32}, with line lengths varying from $25\,\mathrm{km}$ to $300\,\mathrm{km}$. The results are showcased in Fig. 6, where the voltage response of a f-form VSC in each case has been depicted. It is clear that the maximum distance between the f-form and v-form unit must be limited, so that the system stability is preserved. However, it is observed that
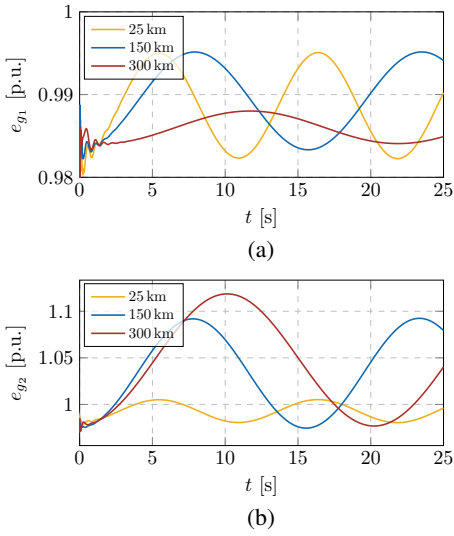
(a)

(b)

Fig. 6: Sensitivity of voltage oscillations to the length of a transmission line: (a) S_{23}; (b) S_{32}.

the location of the loads connection in the network can have a significant impact on the overall response, since the voltage sensitivity is drastically lower for scenario S_{23}. This is due to line dynamics of the shunt admittance, which stabilizes the magnitude of voltage across the load. Since it occurs in the vicinity of the f-form unit in scenario S_{23}, the oscillatory characteristic of the converter voltage is drastically reduced, hence diminishing the effect of the transmission line length.

D. vHIL Results

The presented results are verified through vHIL, by analyzing the system stability for scenario S_{32}. The response of both converters matches the previous analysis, as shown in Fig. 7 through balance of the respective voltage magnitudes and active power outputs. The f-form unit tracks the measured voltage with slight oscillations, whereas the v-form one synchronizes according to the setpoint of the first VSC.
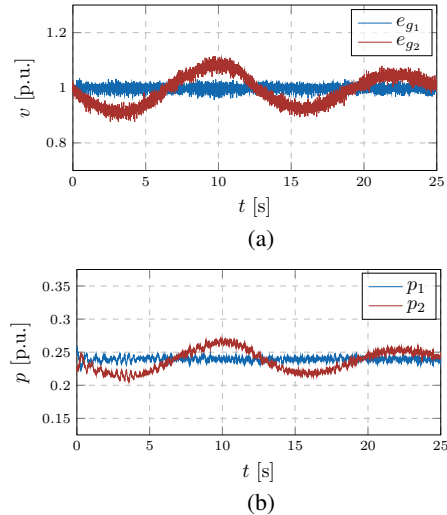

(a)

(b)

Fig. 7: Transient response of the converters in vHIL platform for scenario S_{32}: (a) voltage magnitude; (b) active power.

V. CONCLUSION

In this paper, a new classification of VSC control strategies depending on their mode of operation was presented. A concept of partial grid forming is introduced, which indicates that a 100% inverter-based system can be sustained without a dedicated grid-forming unit. Unlike the existing conventions, the concept is based on partial forming of individual system parameters, distributed across different converter units. Subsequently, a detailed model of VSC was developed in both MATLAB Simulink and vHIL platforms, with a goal of accurately capturing the system dynamics. Finally, using time-domain simulations, the stability of various configuration scenarios was analyzed. The necessary converter and network criteria for providing a stable system under the proposed control concepts have been investigated.

REFERENCES

[1] C. K. Sao and P. W. Lehn, "Control and power management of converter fed microgrids," *IEEE Trans. Power Syst.*, vol. 23, no. 3, pp. 1088–1098, Aug 2008.

[2] A. Mehrizi-Sani and R. Iravani, "Potential-function based control of a microgrid in islanded and grid-connected modes," *IEEE Trans. Power Syst.*, vol. 25, no. 4, pp. 1883–1891, Nov 2010.

[3] F. Katiraei and M. R. Iravani, "Power management strategies for a microgrid with multiple distributed generation units," *IEEE Trans. Power Syst.*, vol. 21, no. 4, pp. 1821–1831, Nov 2006.

[4] G. Diaz, C. Gonzalez-Moran, J. Gomez-Aleixandre, and A. Diez, "Scheduling of droop coefficients for frequency and voltage regulation in isolated microgrids," *IEEE Trans. Power Syst.*, vol. 25, no. 1, pp. 489–496, Feb 2010.

[5] C. L. Moreira, F. O. Resende, and J. A. P. Lopes, "Using low voltage microgrids for service restoration," *IEEE Trans. Power Syst.*, vol. 22, no. 1, pp. 395–403, Feb 2007.

[6] T. Green and M. Prodanović, "Control of inverter-based micro-grids," *Electric Power Systems Research*, vol. 77, no. 9, pp. 1204 – 1213, 2007.

[7] Q.-C. Zhong and T. Hornik, *Control of power inverters in renewable energy and smart grid integration*. John Wiley & Sons, 2012, vol. 97.

[8] Q. Jiang, M. Xue, and G. Geng, "Energy management of microgrid in grid-connected and stand-alone modes," *IEEE Trans. Power Syst.*, vol. 28, no. 3, pp. 3380–3389, Aug 2013.

[9] J. Rocabert, A. Luna, F. Blaabjerg, and P. Rodrguez, "Control of power converters in ac microgrids," *IEEE Trans. Power Electron.*, vol. 27, no. 11, pp. 4734–4749, Nov 2012.

[10] G. M. Foglia, L. Frosio, M. F. Iacchetti, and R. Perini, "Control loops design in a grid supporting mode inverter connected to a microgrid," in *2015 17th European Conference on Power Electronics and Applications (EPE'15 ECCE-Europe)*, Sep 2015.

[11] U. Markovic, P. Aristidou, and G. Hug, "Virtual Induction Machine Strategy for Converters in Power Systems with Low Rotational Inertia," in *IREP Bulk Power System Dynamics & Control Symposium*, Aug 2017.

[12] W. Winter, K. Elkington, G. Bareux, and J. Kostevc, "Pushing the limits: Europe's new grid: Innovative tools to combat transmission bottlenecks and reduced inertia," *IEEE Power and Energy Magazine*, vol. 13, no. 1, pp. 60–74, Jan 2015.

[13] G. Denis, T. Prevost, P. Panciatici, X. Kestelyn, F. Colas, and X. Guillaud, "Review on potential strategies for transmission grid operations based on power electronics interfaced voltage sources," in *2015 IEEE Power Energy Society General Meeting*, Jul 2015.

[14] M.-S. Debry, G. Denis, T. Prevost, F. Xavier, and A. Menze, "Maximizing the penetration of inverter-based generation on large transmission systems: the migrate project," in *6th Solar Integration Workshop*, 2017.

[15] J. A. Taylor, S. V. Dhople, and D. S. Callaway, "Power systems without fuel," *Renewable and Sustainable Energy Reviews*, vol. 57, pp. 1322–1336, 2016.

[16] S.-K. Chung, "A phase tracking system for three phase utility interface inverters," vol. 15, no. 3, pp. 431–438.

[17] Typhoon hil — hardware in the loop testing software and hardware. [Online]. Available: https://www.typhoon-hil.com/